CSMA 2017
13ème Colloque National en Calcul des Structures
15-19 Mai 2017, Presqu'île de Giens (Var)

A Priori Error Estimation for Random Field Generation and a Method to Make Random Generation Scalable in Massively Parallel Implementations

L. de Carvalho Paludor[1], V. Bouvier[1], R. Cottereau[1]

[1] *MSSMat, Centrale Supélec, {luciano.de-carvalho, regis.cottereau}@ecp.fr, {victor.bouvier}@student.ecp.fr*

Résumé — This work analyses the error committed when sampling a random field with the spectral representation method. We conclude the error decreases proportionally to the size of the domain. The problem is that the cost of generation a random field scales as $O(N\log(N))$, where N is the number of points in the simulation. We proposes a subdivision-method that maintain where we can glue together several sample blocks (generated with a $O(N\log(N))$ complexity) into one single field. This allows to have a $O(N)$ scalability of the system, saving much computational effort and suited to massively parallel architectures.
Mots clés — Gaussian-random field sampling, large-scale simulation, parallel computing.

1 Introduction

The use of random fields to represent fluctuating parameters is very common in many scientific domains as micromechanics [1], geomechanics [2, 3] and structural mechanics [4, 5]. With the increase of computational power, we are able to increase the size of simulated domains. As the size of the domain increases, generating these random fields can take more time than the simulation itself. In other words the sampling of the random field can become a computational bottleneck that makes the use of random samples impractical.

In order to tackle this problem we first analyse the existing generation techniques. One generate random using methods in space (direct methods) or in the wave-number domain(spectral methods). Direct methods generate realizations by multiplying a white noise by the square root of the covariance matrix. The calculation of this square root is usually computationally expensive. The Cholesky factorization [6] can be used but scales as (N^3), where N is the number of points of the sample. Alternatively, the generation can be performed in the spectral domain [7, 8]. In this approach the numerical cost is essentially that of computing the inverse Fourier transform, so it scales as $O(N\log N)$ with the Fast Fourier Transform (FFT). However, the parallelization of the FFT algorithm over memory-distributed clusters is not trivial, and involves a large amount of communication between processors. This causes performance loss, and systematically leads to a complexity below the theoretical $O(N\log N)$ when a large number of processors are involved.

We are interested in lowering the computational cost but keep te field quality the same. To minimize the initial cost of computation the most appealing approach is to use spectral-methods along with a FFT. The first part of this work explain how the spectral representation works. To carry on a discussion about quality some error norms are developed in section (3). The forth section shows a new method to build the random sample from smaller samples, making the error on the sample independent of the size of the domain and the last section shows some numerical results.

2 Spectral Representation for random field

The generation of a random field u in a domain D that follows a correlation function $\mathcal{R}$ can be obtained by linear combination of independent and identically distributed (i.i.d.) random variables. Mathematically we can write that $u = \mathcal{G}(\xi)$ for any linear operator $\mathcal{G}$ of $\mathbb{L}^p(D)$ and white noise $\xi = \{\xi(v) : v \in \mathbb{R}^d\}$. A necessary and sufficient condition to this approach is that $\mathcal{G}^\dagger\mathcal{G} = \mathcal{R}$, where we note $\mathcal{G}^\dagger$ the conjugate

transpose of $\mathcal{G}$. In the case of Spectral Representation the operator $\mathcal{G}$ is the Fourier Transform, so we have :

$$\forall x \in D, u(x) = \int_{k\in\mathbb{R}^d} \hat{\mathcal{R}}^{1/2}(k) e^{ik\cdot x} \xi(k) \mathrm{d}k \tag{1}$$

The statistics of first and second order are then $\mathbb{E}[u(x)] = 0$ and $\mathbb{E}[|u(x)|^2] = 1$. And the resulting correlation function is :

$$\mathbb{E}[u(x)\overline{u(y)}] = \int_{(k_1,k_2)\in\left(\mathbb{R}^d\right)^2} \hat{\mathcal{R}}(k_1)\hat{\mathcal{R}}(k_2) e^{ik_1\cdot x} e^{-ik_2\cdot y} \mathbb{E}[\xi(k_1)\xi(k_2)] \mathrm{d}k_1 \mathrm{d}k_2 = \mathcal{R}(x-y) \tag{2}$$

Most of the time, we will take $\xi = \zeta e^{i\phi}$ where ζ is a Gaussian random variable centered and with unitary variance and ϕ is a random variable uniformly distributed in $[0, 2\pi]$.

Aiming numerical tests we are obliged to bound our domain to $D = [0, L]^d$. To make use of the Fourier series expansion one can consider that $\mathcal{R}$ coincides with a S-periodic function $\mathcal{R}_S$ of $\mathbb{R}^d$:

$$\mathcal{R}_S(x_i) = \mathcal{R}_S(x_i + S), \quad \forall x_i \in \mathbb{R}^d \tag{3}$$

We suppose also that $\ell_c \ll L < S$. The Fourier series expansion of $\mathcal{R}_S$, $\forall x \in D$, is $\mathcal{R}_S(x) = \sum_{n\in\mathbb{Z}} \hat{\mathcal{R}}_n e^{i\frac{2\pi}{S}k\cdot x}$ where $\hat{\mathcal{R}}_n = \frac{1}{S^d}\int_D \mathcal{R}_S(x) e^{-i\frac{2\pi}{S}n\cdot x}\mathrm{d}x$. Using $n \in \mathbb{N}^d$ the representation of u becomes then :

$$u(x) = \sum_n \hat{\mathcal{R}}_n^{1/2} \xi(n) e^{i\frac{2\pi}{S}n\cdot x} \tag{4}$$

where $\xi = \{\xi(n) : n \in \mathbb{N}^d\}$ is a white noise of $\mathbb{N}^d$. Since $S \gg \ell_c$ we can assume that : $\hat{\mathcal{R}}_n = \frac{1}{S^d}\int_D \mathcal{R}_S(x) e^{-i\frac{2\pi}{S}n\cdot x}\mathrm{d}x \approx \frac{1}{S^d}\int_{\mathbb{R}^d} \mathcal{R}(x) e^{-i\frac{2\pi}{S}n\cdot x}\mathrm{d}x$.

Another requirement to make simulations possible is that the series of equation (4) need to be truncated at some point. This is acceptable if there is a cutoff wave number $k_{\text{cut}} > 0$ that defines $N_{\text{cut}} = \frac{S}{2\pi}k_{\text{cut}}$, such that $\sum_{n\geq N_{\text{cut}}} |\hat{\mathcal{R}}_n| \approx 0$. It leads to the structured spectral representation of u, first introduced by Shinozuka [7] :

$$u^{\text{STR}}(x) = \sum_{n<N_{\text{cut}}} \hat{\mathcal{R}}_n^{1/2} \xi(n) e^{i\frac{2\pi}{S}n\cdot x} \tag{5}$$

In this paper we will call this representation of u the Structured approach (STR) given we cover the spectrum of u with a uniform step $\Delta k = \frac{2\pi}{L}$.

An efficient way to compute equation (5) is the Fast Fourier Transform. However, it requires our spatial discretization to be equally-spaced and structured. We assume the spatial step defined as $\Delta x = \frac{L}{N_x}$, where N_x is the number of points in the spatial domain $[0, L]$. We can establish a numerical cutoff wave number such that : $k_{\text{cut}}\Delta x = 2\pi$ so $k_{\text{cut}} = \frac{2\pi}{L}N_x$. For a given $m \in [\![0, N_x - 1]\!]^d$, u becomes :

$$u(m\Delta x) = \sum_{n\leq N_x - 1} \hat{\mathcal{R}}_n^{1/2} \xi(n) e^{2i\pi n\cdot m} \tag{6}$$

We can recognize in equation (6) u as the inverse Discrete Fourier Transform (DFT) of a random vector :

$$u^{\text{FFT}}(m\Delta x) = N_x^d \text{DFT}^{-1}\left(\left[\hat{\mathcal{R}}_n^{1/2}\xi(n)\right]_{n\in[\![0,N_x-1]\!]^d}\right) \tag{7}$$

where DFT is the Discrete Fourier Transform operator. The FFT Algorithm provides an optimal way to compute (7).

3 Error Estimation

In this section we will develop two estimators of the correlation function to quantify the quality of the field generated by each method. When sampling a random field u one should truncate the series expansion at some point. If we go far enough the central limit theorem says that we'll obtain Gaussian

first-order marginal as long as ξ is a white noise of $\mathbb{R}^d$. The representation of the spectra is affected by two choices : the way of discretizing k and how many terms we use to represent it (truncation). Precision criteria should be able to quantify the quality of the field based on these two parameters.

We introduce here two error estimators : ε_h and ε_ω. The first, ε_h, takes into account the error on the representation of $\mathcal{R}$ due to discretization. The second, ε_ω, quantifies the error expected in $\mathcal{R}$ for a single realization $\omega \in \Omega$.

3.1 Estimators of $\mathcal{R}$

Before introducing the error estimators we must develop two estimators of the correlation funtion $\mathcal{R}$. For a given $\omega \in \Omega$, we define $\mathbf{R}_\omega$, an estimator of $\mathcal{R}$ computed with a realization u_ω of u :

$$\mathbf{R}_\omega(z) = \frac{1}{|D|}\int_{D_z} u_\omega(x)u_\omega(x+z)\mathrm{d}x,\ \forall z \in D \tag{8}$$

where $|D| = \int_D \mathrm{d}x$. The estimator $\mathbf{R}_\omega$ is a mesure of the ergodicity of the field since to estimate $\mathcal{R}$ from one single realization u_ω we use the spatial average instead of ensemble average. This estimator is a random variable and depends on the realization. The second estimator $\mathbf{R}$ of the correlation function $\mathcal{R}$ takes in account all the realizations u_ω for every $\omega \in \Omega$:

$$\mathbf{R}(z) = \mathbb{E}\left[\omega \mapsto \mathbf{R}_\omega(z)\right] = \frac{1}{|D|}\int_{D_z} \mathbb{E}\left[u(x+z)u(x)\right]\mathrm{d}x \tag{9}$$

This estimator quantifies the impact of using a discretized wave-number space to compute $\mathcal{R}$ with and is deterministic.

3.2 Error decomposition

Using the two estimators $\mathbf{R}_\omega$ and $\mathbf{R}$ we can decompose the total error in two parts : one deterministic and one stochastic. This decomposition, for a given $\omega \in \Omega$ and $p \in \mathbb{N}$, gives us the threshold :

$$\|\mathcal{R} - \mathbf{R}_\omega\|_{\mathbb{L}^p(D)} \leq \|\mathcal{R} - \mathbf{R}\|_{\mathbb{L}^p(D)} + \|\mathbf{R} - \mathbf{R}_\omega\|_{\mathbb{L}^p(D)} \tag{10}$$

The first term on the right-hand side gives the deterioration of the correlation function due to the discretization of the wave-number space. It is deterministic. The Fourier Series Expansion of $\mathcal{R}$, is from an algebraic point view, an optimal projection with respect the $\mathbb{L}^2(D)$-norm. This is the reason why we will use the $\mathbb{L}^2(D)$ norm. We can then conclude our first estimate :

$$\varepsilon_h = \|\mathbf{R} - \mathcal{R}\|_{\mathbb{L}^2(D)} \tag{11}$$

The second term on the right-hand side is realization-dependent and so is a random variable. A well-known result from the Central Limit Theorem ensures that for a random variable X_k the quantity $S_n = \frac{1}{n}\sum_{k=1}^n X_k$ of mean $\bar{S}$ satisfies :

$$\mathbb{P}\left(\left|S_n - \bar{S}\right| \leq \frac{z_\alpha}{\sqrt{n}}\right) = 1 - \alpha \tag{12}$$

where z_α is the quantile of the standard Normal distribution $\mathcal{N}(0,1)$ and $1-\alpha$ is the confidence interval. Putting $S_n = \mathbf{R}_\omega - \mathbf{R}$ we can use this expression to analyse each realization $\omega \in \Omega$. This is our second error estimate ε_ω :

$$\mathbb{P}\left[\|\mathbf{R}_\omega - \mathbf{R}\|_{\mathbb{L}^2(D)} \leq \varepsilon_\omega\right] = 1 - \alpha \tag{13}$$

where $\varepsilon_\omega = \frac{z_\alpha}{\sqrt{n}} + \bar{S}$

3.3 A priori error estimation

By construction of the sample u, there is $\mathbb{E}[u(x)u(x+z)] \approx \sum_{n\leq N_{\text{cut}}} \hat{\mathcal{R}}_{\boldsymbol{n}} e^{i\frac{2\pi}{L}n\cdot z}$. The discretized and truncated $\mathcal{R}$ is (cf. 3.1) our $\mathbf{R}(z) = \sum_{n\leq N_{\text{cut}}} \hat{\mathcal{R}}_{\boldsymbol{n}} e^{i\frac{2\pi}{L}n\cdot z}$. The truncation error is then :

$$\varepsilon_h = \mathcal{R}(z) - \mathbf{R}(z) = \sum_{n>N_{\text{cut}}} \hat{\mathcal{R}}_{\boldsymbol{n}} e^{i\frac{2\pi}{L}n\cdot z}, \forall z \in D, \tag{14}$$

According to the Parseval identity, the $\mathbb{L}^2(D)$-norm could be easily computed as follow :

$$\|\mathcal{R} - \mathbf{R}\|^2_{\mathbb{L}^2(D)} = \sum_{n>N_{\text{cut}}} |\hat{\mathcal{R}}_{\boldsymbol{n}}|^2 \tag{15}$$

The indexer n is a d-dimensional vector. We will note one of the components of n by n_i. Observing that $\hat{\mathcal{R}}_{\boldsymbol{n}} \approx 0$ if any $n_i \to \infty$ we can change the notation from $\hat{\mathcal{R}}_{\boldsymbol{n}}$ to $\hat{\mathcal{R}}_{\boldsymbol{n}_i}$. Suppose there is $\delta > 1$ for which $\lim_{n_i\to\infty} n_i^{\delta}|\hat{\mathcal{R}}_{\boldsymbol{n}_i}|^2 = 0$. In other words $|\hat{\mathcal{R}}_{\boldsymbol{n}_i}|^2$ decreases faster than $\frac{1}{n_i^{\delta}}$. We need for our demonstration a result about the p-series, $\sum_{n=(N_{cut}+1)}^{\infty} \frac{1}{n^{\delta}} \propto O\left(\frac{1}{N_{\text{cut}}^{\delta-1}}\right)$. The right-hand side of Equation (15) for n_i becomes :

$$\sum_{n_i>N_{\text{cut}}} |\hat{\mathcal{R}}_{\boldsymbol{n}_i}|^2 < \left(\sum_{n_i=N_{\text{cut}}+1}^{\infty} \frac{1}{{n_i}^{\delta}}\right) \left(N_{\text{cut}}^{\delta} |\hat{\mathcal{R}}_{N_{\text{cut}}}|^2\right) \approx O\left(N_{\text{cut}} |\hat{\mathcal{R}}_{N_{\text{cut}}}|^2\right) \tag{16}$$

expanding this result for the d components of n we can conclude that

$$\varepsilon_h = ||\mathcal{R} - \mathbf{R}||_{\mathbb{L}^2(D)} = O\left(N_{\text{cut}}^{d/2} |\hat{\mathcal{R}}_{N_{\text{cut}}}|\right) \tag{17}$$

To calculate $\varepsilon_{\omega}^{\text{STR}}$ we should note that for a given $z \in D$ and a given $\omega \in \Omega$,

$$\mathbf{R}_{\omega}(z) = \frac{1}{|D|} \sum_{n_1\leq N_{\text{cut}}} \sum_{n_2\leq N_{\text{cut}}} \sqrt{\hat{\mathcal{R}}_{\boldsymbol{n}_1} \hat{\mathcal{R}}_{\boldsymbol{n}_2}} \left(\xi_{\omega}(n_1)\xi_{\omega}(n_2)\right) e^{i\frac{2\pi}{S}n_2\cdot z} \int_{D_z} e^{i\frac{2\pi}{S}(n_1-n_2)\cdot x} \mathrm{d}x \tag{18}$$

where $\forall n \in \mathbb{N}^d$, $\xi_{\omega}(n)$ is a realization of the random variable $\omega \mapsto \xi_{\omega}(n)$. If the domain $D \gg \ell_c$ $\frac{1}{|D|}\int_{D_z} e^{i\frac{2\pi}{S}(n_1-n_2)\cdot x}\mathrm{d}x$ $\approx \delta(n_1 - n_2)$ and there is :

$$\mathbf{R}_{\omega}(z) = \sum_{n\leq N_{\text{cut}}} \hat{\mathcal{R}}_{\boldsymbol{n}} e^{i\frac{2\pi}{S}n\cdot z} = \mathbf{R}(z) \tag{19}$$

and we can conclude :

$$\forall \omega \in \Omega, \|\mathbf{R}_{\omega} - \mathbf{R}\|_{\mathbb{L}^2(D)} = 0 \tag{20}$$

These developments suggest that the total error is proportional to $O\left(N_{\text{cut}}^{d/2} |\hat{\mathcal{R}}_{N_{\text{cut}}}|^2\right)$ and numerical tests prove this conclusions cf. Fig(1). In other words the error decreases with the increasing of the terms in the wave-number domain (N_k). When using the FFT the number of terms in space (N_x) should also be equal to N_k. We are interested in cases where $L \gg \ell_c$, which results in an enormous N_x. It will usually lead to situations where the the error is much smaller than we need for our simulations. We would like to remind the reader that the computational cost of a FFT is $O(N_x \log(N_x))$ and so having an enormous N_x means that the we are far from the desired scalability.

4 Localization

When the size of the domain, L, is much bigger than the correlation length, ℓ_c, it usually leads to situations that require much more computational power than on single compute can offer. The use of a distributed-memory cluster is then mandatory. It is well known that in parallel computing minimizing the number of communications between processors results in better performance. In the FFT method to generate a random field the question is posed to the whole domain at once, making the distribution between processors a hard task. The localization method comes to overcome this difficulty, minimizing communications. It makes possible to each processor to work independently and, in the end, have a single sample that combines the work of all the processors.

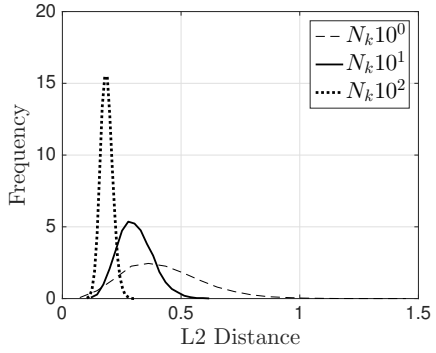

FIGURE 1 – Numerical Results of the error for several values of N_cut. N_k the initial number of terms in the wave-number domain

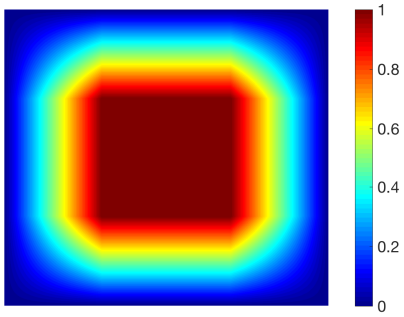

FIGURE 2 – Example of Ψ_i function in a 2D subset. The single-colored square in the middle shows the area not touched by the overlap

Another question that this method addresses is the relation between the error and the size of our domain. As seen in section 3 the errors for the sample are proportional to the inverse of the domain size. It means that one cannot choose independently the size L and the error level (ε_h and ε_ω). Splitting this problem in several sub-problems this issue can be solved. If we are able to sample a part, $\frac{L}{P}$, of the domain at a time and, in the end, glue the parts together each part will need a number of terms N that is proportional to $\frac{L}{P}$ and not the original L. It results in an enormous saving of computational effort since the total number of terms needed to generate the sample decreases drastically.

The correlation function usually has a very strong property called the long distance uncorrelation. This property suggests that one point is only affected by the values on its neighborhood up to a certain distance, usually a few times ℓ_c. Since in our cas $L \gg \ell_c$ we should be able to use this property to divide our domain in several, independent, sub-domains. In the generation methods presented so far this is not the case. Every point, no matter how distant, has its contribution taken into account in the calculation of every other point.

The idea now is to take subsets $D_i \subset D$ that have a non-zero overlapping zone. We will then generate the samples independently over each subset. The challenge is to combine these independent fields in one, statistically homogeneous, continuous field.

In each subset D_i we will define a function $\Psi_i(x)$ that values :

$$\Psi_i(x) = \begin{cases} 1 & \text{if } x \text{ in the interior of the overlapping zone} \\ \sqrt{\psi_i(x)} & \text{if } x \text{ on the overlapping zone} \\ 0 & \text{if } x \text{ in the exterior of the overlapping zone} \end{cases} \tag{21}$$

The functions inside the overlapping zone, $\psi_i(x)$, are partitions of unity and assure the transition from one subset to another. An example of such a function Ψ in 2D domain can be seen in Figure (2). The next subsections will show how using these Ψ_i functions we can combine several independent fields generated in D_i in one statistically homogeneous sample in D.

4.1 Combining d-dimensional subdomains

To combine I independent d-dimensional samples u_i, $\mathcal{N}(0,1)$, over the overlap zone the steps are :

Step 1 (Definition of the domain decomposition and the overlapping area) *Let $(\psi_i)_{i\in I}$ a family of partitions of unity :*

$$\forall x \in D, \sum_{i\in I} \psi_i(x) = 1 \tag{22}$$

$$\tag{23}$$

We note $D_i = \{x \in D, \psi_i(x) \neq 0\}$ and $\hat{D}_{i,j} = D_i \cap D_j$ is the overlapping zone. We introduce the overlap length :

$$\ell_c^{i,j} = \alpha_{i,j}\ell_c = \inf_{\substack{(x,y)\in \hat{D}_{i,j}^2, \\ \psi_i(x)=1, \psi_i(y)=0}} \{||y-x||\} \tag{24}$$

Step 2 (Localized random field's expression) *Let $\forall i \in I, u_i$ a random field generated over D_i. There is $\forall i \in I, u_i = 0$ over $D \backslash D_i$ and u_i is uncorrelated with u_j for $i \neq j$. To ensure the regularity of the localized random field, we compute u_ℓ in this fashion :*

$$u_\ell = \sum_{i\in I} \sqrt{\psi_i} u_i \tag{25}$$

A graphic example of the method applied to a 2D domain can be seen in Figure 3.

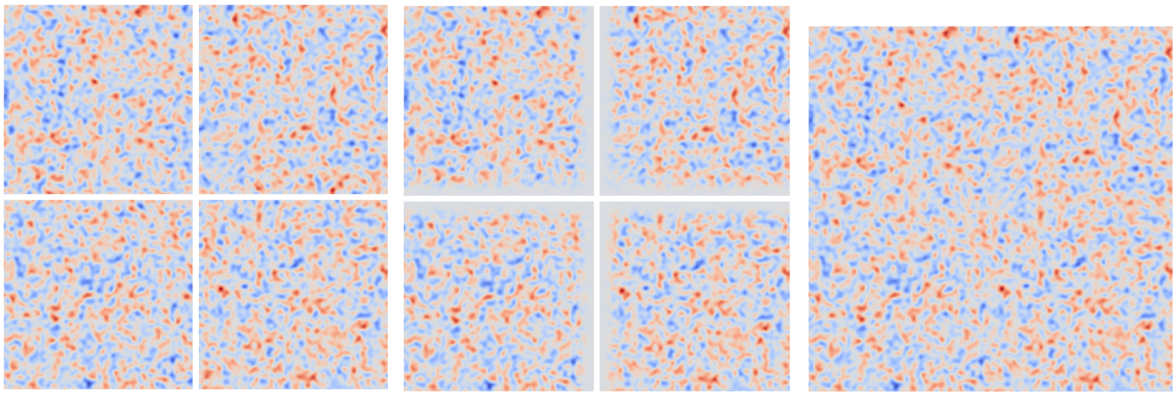

FIGURE 3 – Generation of four independent fields (left), multiplication by the square root of the partitions of unity (center), summation overlapping areas (right).

4.2 Statistics on the overlap zone

The moments of order zero and one remain unaltered :

$$\forall x \in D, \mathbb{E}[u_\ell(x)] = \mathbb{E}\left[\sum_{i\in I} \sqrt{\psi_i(x)} u_i(x)\right] = \sum_{i\in I} \sqrt{\psi_i}\mathbb{E}[u_i(x)] = 0$$

$$\forall x \in D, \mathbb{E}[u_\ell^2(x)] = \sum_{(i,j)\in I^2} \sqrt{\psi_i(x)}\sqrt{\psi_j(x)}\mathbb{E}[u_i(x)u_j(x)] = \sum_{i\in I} \psi_i(x)\mathbb{E}[u_i(x)^2] = 1$$

Lets take a look in how localization distorts the estimator $\mathbf{R}$. We will focus on the estimator $\mathbf{R}_\ell$ where $\forall z \in D, \mathbf{R}_\ell(z) = \frac{1}{|D|}\int_{x\in D_z} \mathbb{E}\left[u_\ell(x)u_\ell(x+z)\right] \mathrm{d}x$.

$$\forall z \in D, \mathbf{R}_\ell(z) = \frac{1}{|D|}\int_{x\in D_z} \mathbb{E}\left[\sum_{(i,j)\in I^2} \sqrt{\psi_i(x)\psi_j(x+z)}u_i(x)u_j(x+z)\right]\mathrm{d}x \tag{26}$$

$$= \frac{1}{|D|}\int_{x\in D_z} \sum_{(i,j)\in I^2} \sqrt{\psi_i(x)\psi_j(x+z)}\mathbb{E}[u_i(x)u_j(x+z)]\mathrm{d}x \tag{27}$$

$$= \frac{1}{|D|}\sum_{i\in I}\int_{x\in D_z} \sqrt{\psi_i(x)\psi_i(x+z)}\mathbb{E}[u_i(x)u_i(x+z)]\mathrm{d}x \tag{28}$$

The equation (28) is obtained because the fields u_i and u_j are generated independently for $i \neq j$ so : $\mathbb{E}[u_i(x)u_j(x+z)] = \mathbb{E}[u_i(x)]\mathbb{E}[u_j(x+z)] = 0$. For an arbitrary $i \in I$, the Equation (28) is obtained because the statistical properties are the same for all the subdomains. The correlation function is affected by a factor $\sqrt{\psi_i(x)\psi_i(x+z)}$. This term should go to one as long as $\psi_i(x)$ does not fluctuates a lot over the distance of one or some correlation lengths ℓ_c. The expression of the difference between $\mathbf{R}_\ell$ and $\mathbf{R}$; $\forall z \in D$,, can be expressed as :

$$\mathbf{R}_\ell(z) - \mathbf{R}(z) = \frac{1}{|D|}\sum_{i\in I}\int_{x\in D_z}\left(\sqrt{\psi_i(x)}\left(\sqrt{\psi_i(x)} + \varepsilon_{\psi_i(x)}(z)\right)\right)\mathbb{E}[u_i(x)u_i(x+z)]\mathrm{d}x - \mathbf{R}(z) \tag{29}$$

$$= \frac{1}{|D|}\int_{x\in D_z}\left(\sum_{i\in I}\psi_i(x)\right)\mathbb{E}[u_i(x)u_i(x+z)]\mathrm{d}x - \mathbf{R}(z)$$

$$+ \frac{1}{|D|}\int_{x\in D_z}\sum_{i\in I}\sqrt{\psi_i(x)}\varepsilon_{\psi_i(x)}(z)\mathbb{E}[u_i(x)u_i(x+z)]\mathrm{d}x \tag{30}$$

$$= \frac{1}{|D|}\int_{x\in D_z}\sum_{i\in I}\sqrt{\psi_i(x)}\varepsilon_{\psi_i(x)}(z)\mathbb{E}[u_i(x)u_i(x+z)]\mathrm{d}x \tag{31}$$

Where $\varepsilon_{\psi_i(x)}(z)$ is the difference $\varepsilon_{\psi_i(x)}(z) = \sqrt{\psi_i(x+z)} - \sqrt{\psi_i(x)}$. Making a Taylor-Lagrange expansion around x of $\sqrt{\psi_i(x+z)}$ a well-known result ensures :

$$\forall z \in D, \left|\varepsilon_{\psi_i(x)}(z)\right| \leq \sup_{x\in D}\left|\left|\nabla\sqrt{\psi_i}|_x\right|\right| ||z|| \tag{32}$$

Remarking, $\forall i \in I, \forall x \in D, 0 \leq \sqrt{\psi_i(x)} \leq 1$, $\forall i \in I$, there is $\mathcal{M}_i$ such that :

$$\left|\sqrt{\psi_i(x)}\varepsilon_{\psi_i(x)}(z)\right| \leq \mathcal{M}_i||z|| \tag{33}$$

If we stablish a z_{cut} where $\forall||z|| > z_{cut}, \mathbf{R}(z) \approxeq 0$. Finally we can conclude :

$$||\mathbf{R}_\ell - \mathbf{R}||_{\mathbb{L}^\infty(D)} \leq \sum_{i\in I}\mathcal{M}_i \sup_{||z||\leq z_{cut}} ||z||\mathbf{R}(z) \tag{34}$$

The optimal choice of ψ is not discussed in this article. Considerations about smoothness of the generation field should be taken into account. In our examples we used $\psi_i = \prod_{n=1}^{d}\frac{1}{2}\left(1 + cos\left(\frac{\pi}{2}\left(1 + \frac{x_n^*}{\alpha}\right)\right)\right)$, where x_n^* is the coordinate that measures the distance on the overlap in each n-direction. It values $x_n^* = 0$ when it is on the interior limit of the overlapping zone and $x_n^* = \alpha$ on the exterior limit.

4.3 Numerical Results

We are now interested at what happens when we perform calculations in several processors. When paralelizing we would like that two times more processors could compute a domain that has two times more points (keeping the density of points constant). The linear scalability of the FFT method with localization suggest that it can be possible. The challenge here is that the communication between the processors have to follow the linear scalability. In the implementation the MPI standard was used because we aim problems that are big enough to need a distributed memory architecture. At each iteration we multiply by two the number of points on the grid and we double the number of processors. Results show

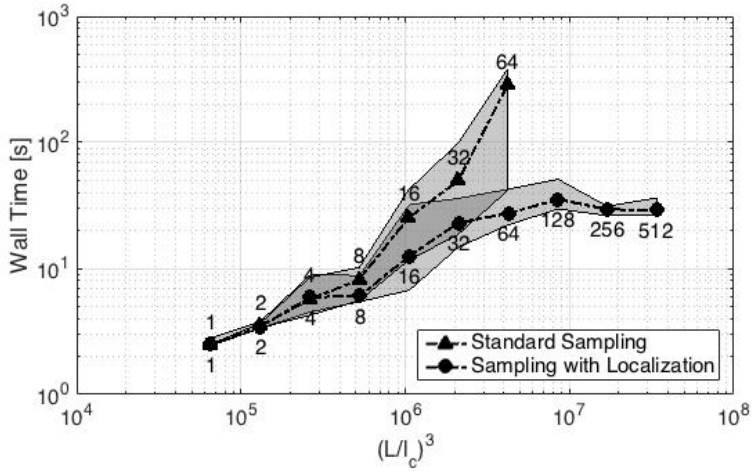

FIGURE 4 – Weak Scaling without localization and with localization 3D cases. The number on each point is the number of processors.

the generation time, from reading the input to writing the output files, in Figure 4. The shadow indicates the span between the best and worst case in each simulation.

We chose to test on the 3D case because it is where the real challenge is. In 3D the computational cost grows rapidly and, when using several processors, the interface between processors is larger.

The difference between the problem using the localization approach and the standard are clear. An expected and yet remarkable phenomena is the plateau revealed in the localization method. It suits the methods to solve large scale problems. We tested the FFT with localization CentraleSupélec cluster, Igloo, (Intel Xeon X7542 2.66Ghz/800 cores) and with 512 processors (8x8x8 processors grid) we are able to generate a 300 ℓ_c cube in 16 seconds (Figure 5).

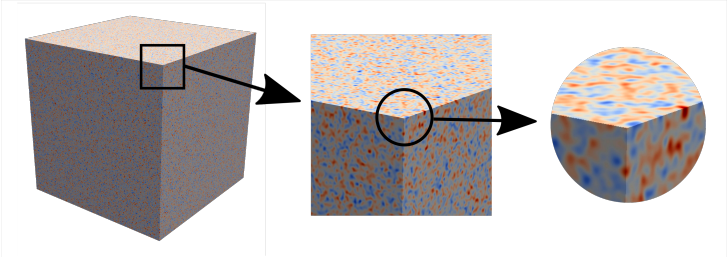

FIGURE 5 – Simulation of a $300\ell_c \times 300\ell_c \times 300\ell_c$ field over 512 Processors.

Références

[1] L. Huyse and M. A. Maes. Random field modeling of elastic properties using homogenization. *J. Engr. Mech.*, 127(1) :27–36, 2001.

[2] R. Popescu, G. Deodatis, and A. Nobahar. Effects of random heterogeneity of soil properties on bearing capacity. *Prob. Engr. Mech.*, 20 :324–341, 2005.

[3] R. Cottereau, D. Clouteau, and C. Soize. Probabilistic impedance of foundation : impact of the seismic design on uncertain soils. *Earthquake Engr. Struct. Dyn.*, 196(17-20) :899–918, 2007.

[4] S.-K. Choi, R. V. Gandhi, and R. A. Canfield. *Reliability-based structural design*. Springer, 2006.

[5] D. Clouteau, R. Cottereau, and G. Lombaert. Dynamics of structures coupled with elastic media – a review. *J. Sound Vib.*, 332(10) :2415–2436, 2013.

[6] H. Rue. Fast sampling of Gaussian Markov random fields. *J. Roy. Stat. Soc.*, B63 :325–338, 2001.

[7] M. Shinozuka and C.-M. Jan. Digital simulation of random processes and its applications. *J. Sound Vib.*, 25(1) :111–128, 1972.

[8] M. Shinozuka and G. Deodatis. Simulation of stochastic processes by spectral representation. *Appl. Mech. Rev.*, 44(4) :191–205, 1991.